Journal of Applied Physics

RESEARCH ARTICLE | FEBRUARY 24 2026

An analytic decomposition approach to modeling evanescent transient plane waves with an illustrative application to acoustics at a fluid–fluid interface FREE

Philippe Gatignol ; Catherine Potel ; Michel Bruneau

J. Appl. Phys. 139, 084902 (2026)
https://doi.org/10.1063/5.0307794

Journal of Applied Physics ARTICLE pubs.aip.org/aip/jap

An analytic decomposition approach to modeling evanescent transient plane waves with an illustrative application to acoustics at a fluid–fluid interface

Cite as: J. Appl. Phys. **139**, 084902 (2026); doi: 10.1063/5.0307794
Submitted: 18 October 2025 · Accepted: 29 January 2026 ·
Published Online: 24 February 2026

Philippe Gatignol,[1,a)] Catherine Potel,[2,b)] and Michel Bruneau[2]

AFFILIATIONS

[1]Laboratoire Roberval, Université de Technologie de Compiègne, Compiègne, France
[2]Laboratoire d'Acoustique de l'Université du Mans (LAUM), UMR 6613, Institut d'Acoustique—Graduate School (IA-GS), CNRS, Le Mans Université, Le Mans, Cedex 9 72085, France

[a)]**Present address:** 13, avenue du Centre, Montgeron F-91230, France.
[b)]**Author to whom correspondence should be addressed:** catherine.potel@univ-lemans.fr

ABSTRACT

This work introduces an analytic decomposition approach for transient plane waves, broadly applicable to their interaction with layered media in linear physics. The time-domain signal, assumed to be analytic, is extended into the complex plane and then analytically decomposed into two parts, in a manner reminiscent of the Wiener–Hopf technique. The method directly provides the Hilbert transform of the signal and the expressions of the complex fields without resorting to Fourier transforms or the calculation of singular integrals. It applies to a wide class of functions capable of simulating most realistic signals, such as multi-frequency oscillatory signals of limited duration, and is particularly relevant whenever certain fields become evanescent. An illustrative application to acoustics at a fluid–fluid interface offers deeper physical insight than previously available, particularly regarding the processes that generate precursor and successor phenomena in the reflected and transmitted fields, taking advantage of both the simplicity and the effectiveness of the method.

I. INTRODUCTION

In this article, we introduce an analytical resolution method for the computation and representation of the physical fields arising in certain linear wave-propagation phenomena of a transient nature with finite temporal support. Such situations occur in many areas of physics, including fluid acoustics,[1,2] optics and electromagnetic wave propagation,[3] acoustics in solids,[4,5] and layered media and seismic waves.[6,7]

The fields are assumed to be deterministic and amenable to a description as superpositions of plane waves. The propagation domain consists of several media separated by planar interfaces, thereby forming a multilayered structure. Each plane wave is defined by a signal function $f(X)$, where X is initially a real variable. Depending on the propagation medium, some waves may become evanescent, in which case the argument X takes complex values.

For monochromatic fields, the signal function is sinusoidal, and the computation is carried out by decomposing the sine function into a sum of complex exponentials. This representation makes it possible to account for evanescent contributions and to express boundary conditions at infinity in a simple manner.

In the case of time-limited transient fields, the usual approach consists in starting from elementary signal functions, such as the rectangular pulse or, more generally, piecewise continuous oscillatory signals, chosen so that their Fourier transforms can be determined explicitly. The Fourier transform is then decomposed into causal and anti-causal parts, and the time-domain field is recovered by inverse Fourier transforms. This procedure leads to the integral expression of the analytic signal associated with the original signal function. It involves the Hilbert transform of this function, which is expressed as a Cauchy principal value integral.

An alternative to this approach is to compute the Hilbert transform directly by means of a convolution integral in the sense of distributions (see, for example, Ref. 8).

This integral approach suffers from several drawbacks. In addition to the need to select suitably adapted signal functions and given the truncation and sampling errors inherent in the numerical evaluation of Fourier integrals, such signal functions may lead to artifacts devoid of physical meaning, owing to the singular behavior of the Hilbert transform for signal functions exhibiting discontinuities. Moreover, this method does not allow one to determine directly evanescent fields, whose spatiotemporal arguments take complex values.

We, therefore, propose an alternative approach based on the direct analytical decomposition of the signal function, thereby generalizing the formalism of monochromatic complex fields. The method relies on the assumption of analyticity of the field functions: The signal function $f(X)$ is assumed to be defined and analytic for all real values of X. Such a function can be extended, in the complex plane of the variable Z associated with the real variable X, to a function $f(Z)$ that is holomorphic in a neighborhood of the real axis. It is further assumed that, as in the case of the sine function, $f(Z)$ admits an analytical decomposition, that is, it can be expressed as the sum of two functions, one holomorphic in the upper complex half-plane and the other in the lower half-plane. In addition, each of these functions must be bounded at infinity in the corresponding half-plane and tend to zero for large values of $|\mathrm{Im}(Z)|$. Under these assumptions, the analytical decomposition is unique. The determination of the physical fields then proceeds in the same manner as in the monochromatic case.

The set of functions satisfying these hypotheses forms a vector space to which the sine function belongs. It contains a large subspace of functions constructed from rational and trigonometric functions, for which the analytical decomposition can be determined directly using a procedure analogous to the Wiener–Hopf method employed in frequency-domain diffraction problems (see Ref. 9 for the theory and Refs. 10, 11 for examples).

Based on these functions, the decomposition method offers a number of advantages. By an appropriate choice of the signal function, it is possible to account for the finite-duration transient character of the plane wave. The method yields explicit expressions for the various fields, whether propagative or evanescent, in the form of sums of terms involving standard functions, without any approximation other than those required for the evaluation of these functions. This avoids any approximate computation of Fourier or Hilbert integrals. As a result, the method is easy to implement numerically and leads to very short computation times, even when the number of terms is very large (of the order of one thousand in the fluid–fluid interface example considered in this paper). For comparison purposes, the method also allows one to approximate with high accuracy the theoretical signal functions commonly used in the literature and mentioned above, by regularizing them and thereby avoiding the nonphysical singularities they may induce.

The introduction of complex fields also makes it possible to address energetic quantities in the same manner as in the monochromatic case, by decomposing instantaneous quantities into active and complementary parts. This energetic decomposition is used in the interface example to explain the emergence of a precursor under supercritical incidence, as reported by several authors.

Although the present work is primarily oriented toward acoustic waves in fluids or in elastic solids, whether isotropic or not, the proposed method applies to other types of waves, in particular, electromagnetic waves.

The method is presented in full generality in the Secs. II and III. Section II recalls the necessity of considering functions with complex arguments in the presence of evanescent fields. The analyticity assumptions on the signal functions and their analytical decomposition are specified. The connection with analytic signal theory and the Hilbert transform is established, while generalizing these notions to complex signals. Section III details the implementation of the method for physical configurations involving multiple media and multiple interfaces. The linear differential system with real coefficients, consisting of the propagation equations for the various waves in each medium together with the continuity conditions at the interfaces, provides the basis for deriving the various physical (real) propagative and evanescent fields through the use of complex fields.

Section IV is devoted to the construction of the subspace of signal functions based on rational and trigonometric functions. The approximation of discontinuous functions, such as the rectangular pulse, is discussed.

For pedagogical purposes, the method is then applied, starting from these signal functions, to the simple case of a plane wave interacting with a planar interface separating two fluids. This case is chosen for its relative simplicity, while more complex configurations, including multilayered and solid media, are left for future studies.

The method, together with the interface conditions, is detailed in Sec. V. Explicit results are presented in Sec. VI. In particular, under supercritical incidence, the emergence of a precursor in the reflected field is demonstrated and explained, both from a mathematical standpoint and on more physical grounds by introducing energetic quantities computed from the complex fields.

II. THE METHOD OF ANALYTIC DECOMPOSITION

The analytic decomposition of a function is a process similar to the additive separation of the function into its even and odd, or real and imaginary parts. Below, we present this decomposition concept and its close connection with the Hilbert transformation and the associated analytic signal. We will highlight a broad class of functions that are analytically decomposable in this sense. However, characterizing all decomposable functions is beyond the scope of this paper. Readers interested in the theory of half-plane holomorphic functions may refer to Ref. 12.

A. Occurrence of complex arguments

Plane waves are described by introducing a signal function $f(X)$ that depends on a real variable X. The latter is a linear function of the (non-dimensional) space (x, y, z) and time (t) coordinates. We will express it in the form

$$X = m(\alpha x + \beta y + \gamma z) - t, \text{ with } \alpha^2 + \beta^2 + \gamma^2 = 1, \qquad (1)$$

where $\mathbf{n}(\alpha, \beta, \gamma)$ is the unit propagation vector and $m = 1/c$ is the inverse sound velocity of the medium, such that $\mathbf{m} = m\,\mathbf{n}$ is the so-called "slowness vector" of the wave in the direction $\mathbf{n}$. For a propagating plane wave, the argument X in (1) is real-valued, and *a priori*, the function $f(X)$ is real. This will be the case for the given incident field in the example studied in Sec. V, where x and y are the spatial coordinates in the plane of an interface between two media while z denotes the coordinate normal to this interface directed outward from the incident medium.

But if the wave is evanescent, the argument X becomes complex-valued, which we denote by adding a "hat": $\hat{X}$. Indeed, the components α, β, and γ of the unit propagation vector are no longer all real. In the example discussed in Sec. V, the component γ becomes imaginary in the half-space $z \geq 0$, i.e., $\hat{\gamma} = i\gamma''(\gamma'' > 0)$, so that we have

$$\hat{X} = m(\alpha x + \beta y + i\gamma'' z) - t, \forall\, x, y, t \in \mathbb{R}, \forall\, z \geq 0. \tag{2}$$

The function $f(X)$, with real variable X, is no longer appropriate. We must introduce the complex variable $Z = X + iY$ and consider the possibility of extending the function $f(X)$ to a complex function $\hat{f}(Z)$ in the complex plane. Then, the values of the field function $\hat{f}(Z = \hat{X})$ become complex, and this may also occur for other field functions of the problem, even if they describe propagating waves. It is important to understand that, while Z denotes the current variable of the function $\hat{f}(Z)$, $\hat{X}$ represents the value of Z as it appears in the expression of the evanescent fields, according to Eq. (2).

B. Introduction of complex field functions

Under these circumstances, the analytic decomposition of the field functions will form the basis of the study. For this purpose, we will assume that the original signal function $f(X)$ satisfies three hypotheses.

1. First hypothesis (a)

Hypothesis (a). The function $f(X)$ is analytic on the whole real line $\mathbb{R}$, which implies that: (i) $f(X) \in C_\infty(\mathbb{R})$; (ii) $\forall X_0 \in \mathbb{R}$ the Taylor series of $f(X)$ at X_0 converges in a non-zero interval I_{X_0}; (iii) in this interval, the sum of the Taylor series equals $f(X)$.

As a consequence, according to the theory of analytic continuation of holomorphic functions of the complex variable $Z = X + i\,Y$ (see Ref. 13, chapter IV, and Refs. 14–16), it follows that there exists an analytic function $\hat{f}(Z)$, which is holomorphic in some neighborhood Ω of the real axis $\mathbb{R}$, in that sense that Ω contains a strip B_ε: $|\mathrm{Im}(Z)| < \varepsilon$. This analytic extension $\hat{f}(Z)$ is unique and is such that $\hat{f}(Z) = f(X)$ for $Z = X \in \mathbb{R}$. As a result, we can now make sense of the expression $f(X)$ when the argument X takes complex values $Z = \hat{X} \in B_\varepsilon$, such as those given by expression (2).

2. Second hypothesis (b)

However, as already mentioned, this complex propagation variable $\hat{X}$ can take any value in one of the complex half-planes $\mathrm{Im}\{Z\} \geq 0$ or $\mathrm{Im}\{Z\} \leq 0$. In general, the domain Ω does not contain any of these half-planes. For this reason, we introduce a second hypothesis related to the signal function or more precisely to its extension $\hat{f}(Z)$.

Hypothesis (b). The analytic extension $\hat{f}(Z)$ can be decomposed as a sum of two terms,

$$\hat{f}(Z) = \hat{f}^+(Z) + \hat{f}^-(Z), \tag{3}$$

where $\hat{f}^+(Z)$ is holomorphic in a half-plane $\mathrm{Im}\{Z\} > -\varepsilon$ and $\hat{f}^-(Z)$ is holomorphic in a half-plane $\mathrm{Im}\{Z\} < \varepsilon$, with $\varepsilon > 0$.

Such decomposition is well known in Wiener–Hopf techniques. Reference 10 provides a clear explanation of the process, along with a very clear figure (Fig. 2 of Ref. 10) illustrating the two half-planes of holomorphy.

Under this hypothesis, we can consider the values of one of these two functions when its argument $Z = \hat{X}$ takes values in one of these two half-planes.

3. Third hypothesis (c)

However, the behavior at infinity of these two functions is not specified, meaning that writing the decreasing condition of evanescence for the associated field is not yet possible. For this to be feasible, we must introduce a third hypothesis related to the behavior at infinity of the terms of the decomposition (3).

Let us first note that if hypotheses (a) and (b) are satisfied by the function $f(X)$, the same holds for all its derivatives, with the analytic decomposition of each of them being obtained by a simple derivation of the decomposition (3). The third hypothesis needed is then stated as follows:

Hypothesis (c). Both terms of the decomposition (3) and their derivatives, at least up to the second order, are bounded at infinity in their respective half-plane of holomorphy, and they tend toward 0 at least as $1/|Z|$ as $|\mathrm{Im}\{Z\}| \to +\infty$ in this half-plane.

A fundamental consequence of this third hypothesis (c) is that the additive decomposition (3) of the function $\hat{f}(Z)$, if it exists, is unique. This result is obtained by applying Liouville's theorem, which is stated as follows (see Ref. 13, Sec. 2.51): "A function that is analytic for all finite values of Z and is bounded, is a constant."

Under these three hypotheses, we refer to the terms $\hat{f}^+(Z)$ and $\hat{f}^-(Z)$ as the *upper* and *lower parts* of $\hat{f}(Z)$, or equivalently of the signal function $f(X)$, and denote by H^+ and H^- the sets to which they belong, respectively. The set of these decomposable functions $\hat{f}(Z)$ forms a vector space H over the field $\mathbb{C}$, and the sets H^+ and H^- are supplementary subspaces of H (due to the uniqueness of the decomposition) so that

$$\mathrm{H} = \mathrm{H}^+ \oplus \mathrm{H}^-. \tag{4}$$

C. Specific expression for the argument $\hat{X}$, translation properties

When the argument X takes complex values according to Eq. (2), which can be rewritten in the more condensed form

$$\hat{X} = \xi + \hat{\zeta}, \xi = m(\alpha x + \beta y) - t, \hat{\zeta} = i\gamma'' z, \tag{5}$$

the extension function $\hat{f}(\hat{X})$ only makes sense if $|\mathrm{Im}(\hat{X})| = \gamma''|z| < \varepsilon$. For its upper part $\hat{f}^+(\hat{X})$, we must have the condition $\mathrm{Im}(\hat{X}) > -\varepsilon$, and for $\hat{f}^-(\hat{X})$, the condition $\mathrm{Im}(\hat{X}) < \varepsilon$. From this, we deduce the following translation properties for the extension function and its upper and lower parts.

If $\hat{f}(Z) \in \mathrm{H}$, then $\hat{f}(Z+\eta) \in \mathrm{H}$ for $\eta \in \mathbb{R}$. If $\hat{f}^+(Z) \in \mathrm{H}^+$, then $\hat{f}^+(Z+\hat{\eta}) \in \mathrm{H}^+$ for $\mathrm{Im}(\hat{\eta}) \geq 0$. If $\hat{f}^-(Z) \in \mathrm{H}^-$, then $\hat{f}^-(Z+\hat{\eta}) \in \mathrm{H}^-$ for $\mathrm{Im}(\hat{\eta}) \leq 0$.

D. Case of a real-valued signal function

1. Expression of the signal function in terms of $\hat{f}^+$

The functions in H^+ or H^- all possess the properties required to represent evanescent fields in a complex form in unbounded regions of space. It remains to determine the relationship that directly links them to the initial signal function $f(X)$. Returning to the case where this signal function is real-valued, we can assert, according to the Schwarz symmetry principle, also called the principle of reflection (see Ref. 13, Sec. 4.5), that the holomorphic domain Ω of its extension $\hat{f}(Z)$ is symmetric with respect to the real axis and that this function satisfies the identity $\hat{f}(Z) = [\hat{f}(Z^*)]^*$, where Z^* denotes the complex conjugate of Z. We can easily deduce, by applying this identity to the decomposition (3) and using the uniqueness of the analytic decomposition, the (equivalent) relations,

$$\hat{f}^+(Z) = [\hat{f}^-(Z^*)]^*, \ \hat{f}^-(Z) = [\hat{f}^+(Z^*)]^*. \tag{6}$$

For $Z = X \in \mathbb{R}$, we obtain

$$\hat{f}^+(X) = [\hat{f}^-(X)]^*, \ \hat{f}^-(X) = [\hat{f}^+(X)]^*. \tag{7}$$

Thus, for real X, we have the following expression for the signal function:

$$f(X) = \hat{f}^+(X) + [\hat{f}^+(X)]^* = 2\,\mathrm{Re}\{\hat{f}^+(X)\}. \tag{8}$$

2. Connection with the real Hilbert transform and analytic signal

The decomposition (3) of the complex function $\hat{f}(Z)$ allows us to define another function, namely,

$$\hat{f}_H(Z) = \hat{f}^+(Z) - \hat{f}^-(Z). \tag{9}$$

This companion function can be aptly called the *complex Hilbert transform* of $\hat{f}(Z)$. It belongs to the vector space H, with the property

$$\hat{f}_{H\hat{H}}(Z) = \hat{f}(Z). \tag{10}$$

In the case of a real-valued signal function $f(X)$, relation (7) shows that $\hat{f}_H(Z)$ has imaginary values for $Z = X \in \mathbb{R}$:

$$\hat{f}_{\hat{H}}(X) = i f_H(X). \tag{11}$$

It can be shown, using the Cauchy theorem in the complex plane Z (see Ref. 13, Sec. 2.3), that the real function $f_H(X)$ is the usual Hilbert transform of $f(X)$, with the classical property $f_{HH}(X) = -f(X)$ from Eqs. (10) and (11).

As a consequence, we have the following expressions for the usual analytic signals:

$$\hat{f}_A(X) = f(X) + i f_H(X) = 2\hat{f}^+(X), \ \hat{f}_B(X) = f(X) - i f_H(X) = 2\hat{f}^-(X). \tag{12}$$

E. Summary of Sec. II

We describe the plane waves of the various physical fields by introducing signal functions $f(X)$ with real or complex values, where X is a linear function of space and time variables. The functions $f(X)$ are assumed to be analytic for all real values of X, and such that their complex extension $\hat{f}(Z)$, holomorphic in a neighborhood of the real axis, can be decomposed into the sum of two terms: The upper part $\hat{f}^+(Z)$, holomorphic in the half-plane $\mathrm{Im}(Z) > -\varepsilon$, bounded in this half-plane, and tending to zero as $\mathrm{Im}(Z) \to +\infty$; and the lower part $\hat{f}^-(Z)$, possessing analogous properties in the half-plane $\mathrm{Im}(Z) < +\varepsilon$. This decomposition is unique. If the function $f(X)$ is real-valued, it can be expressed directly in terms of the real part of its upper part $\hat{f}^+(Z)$, according to relation (8).

III. IMPLEMENTATION OF THE METHOD FOR TRANSIENT PLANE WAVES (MULTILAYERED MEDIA)

As a basic situation, we consider a transient plane wave interacting with a multilayered structure S. The structure S consists of several continuous fluid or solid media $M_q (q = 0, \ldots, Q)$ separated by one or more plane interfaces I_s, all perpendicular to the Oz axis (see example in Sec. V). The incident plane wave propagates in the medium M_0 and meets the first interface at a given angle of incidence.

A process of successive reflections occurs at the interfaces. The interaction phenomenon involves several physical fields $\varphi_{qr}(x, y, z; t)$ in each medium M_q (for example, acoustic pressure or velocity potential): incident and reflected fields, transmitted field or intermediate fields in a layer, longitudinal and transversal waves for an elastic medium, etc. In order to simplify the mathematical notation, we denote all of these field functions as φ_j, $(j = 0, \ldots, J)$, where φ_0 represents the given incident field.

Each of these functions φ_j must satisfy a specific wave equation,

$$E_j\{\varphi_j\} \equiv \Delta\varphi_j - m_j^2 \frac{\partial^2 \varphi_j}{\partial t^2} = 0, \tag{13}$$

where $m_j = 1/c_j$ depends on the nature of the wave and on the medium where it propagates.

All the field functions φ_j are linked by the continuity conditions at the interfaces I_s. Each of these conditions involves a given subset of $\{\varphi_j\}$ and takes the form of a linear operator denoted I with real coefficients, which may be a differential operator if it concerns potential fields. Taken together, these conditions involve all the functions φ_j. We note this global linear system as

$$I\{\varphi_0, \varphi_1, \ldots, \varphi_J\} = 0. \tag{14}$$

Since the functions φ_j represent plane waves and are solutions of Eq. (13), they take the form

$$\varphi_j = f_j(X_j),\ X_j = m_j(\alpha_j x + \beta_j y + \gamma_j z) - t + \eta_j, \tag{15}$$

where η_j represents a delay term depending on successive reflections. The function $f_0(X_0)$ represents the incident field, which is assumed to be known. The other functions $f_j(X_j)$ are the unknowns of the problem.

As a necessary condition for Eq. (14) to hold, all the arguments X_j depend on the same interface spatiotemporal variable ξ, so that they can be written as

$$X_j = \xi + \zeta_j,\ \xi = m(\alpha x + \beta y) - t,\ \zeta_j = m_j\gamma_j z + \eta_j. \tag{16}$$

If all the fields in the problem are propagative, all X_j are real, and since the interface operators have real coefficients, all the associated signal functions $f_j(X_j)$ are real-valued. In this case, the problem can be solved directly using these real functions without introducing complex fields.

On the other hand, if at least one of the fields φ_j is evanescent, its argument X_j becomes complex,

$$\hat{X}_j = \xi + \hat{\zeta}_j,\ \hat{\zeta}_j = m_j\hat{\gamma}_j z + \hat{\eta}_j. \tag{17}$$

In this case, most other arguments become complex, except for that of the incident field and a few others. Thus, solving the problem requires the introduction of complex field functions, which means that the signal functions $f_j(X)$ must satisfy the hypotheses (a)–(c) mentioned above.

One might think that the choice of the complex function depends on the values of their arguments $\hat{X}_j$, namely, the extension function $\hat{f}_k(Z)$ if $Z = X_k$ is real, the upper part $\hat{f}_\ell^+(Z)$ if $\mathrm{Im}\{\hat{X}_\ell\} \geq 0$, and the lower part $\hat{f}_{\ell'}^-(Z)$ if $\mathrm{Im}\{\hat{X}_{\ell'}\} \leq 0$. However, it can be easily shown that such a choice is impossible. Indeed, since the operator I has real coefficients, Eq. (14) must be verified by these complex fields. Substituting the complex functions into this linear system would yield

$$I\left\{\hat{f}_k(\xi + \zeta_k);\ \hat{f}_\ell^+(\xi + \hat{\zeta}_\ell);\ \hat{f}_{\ell'}^-(\xi + \hat{\zeta}_{\ell'})\right\} = 0. \tag{18}$$

The functions $\hat{f}_k(Z)$ can be split into their upper and lower parts, and due to the linearity of the operator I, we can write

$$I\left\{\hat{f}_k^+(\xi + \zeta_k);\ \hat{f}_\ell^+(\xi + \hat{\zeta}_\ell);\ 0\right\} + I\left\{\hat{f}_k^-(\xi + \zeta_k);\ 0;\ \hat{f}_{\ell'}^-(\xi + \hat{\zeta}_{\ell'})\right\} = 0. \tag{19}$$

Using the translation properties and hypothesis (c), we deduce that, for the extension $\xi \to Z$, the first term belongs to H^+ and the second to H^-. Due to the uniqueness of the analytic decomposition, it follows that Eq. (19) splits into two equations,

$$I\left\{\hat{f}_k^+(\xi + \zeta_k);\ \hat{f}_\ell^+(\xi + \hat{\zeta}_\ell);\ 0\right\} = 0,\ I\left\{\hat{f}_k^-(\xi + \zeta_k);\ 0;\ \hat{f}_{\ell'}^-(\xi + \hat{\zeta}_{\ell'})\right\} = 0. \tag{20}$$

Neither of these two equations solves the problem.

Consequently, solving the problem requires that all complex fields be represented by analytic functions of the same type—either the upper or the lower parts of the signal functions. Considering the behavior of the ultimate field φ_J in the last medium M_Q, which is assumed to extend to infinity, we see that this field must tend to 0 if it is evanescent. Due to the form of the arguments $\hat{X}_j$, it follows that we must choose the upper part $\hat{f}_J^+(\hat{X}_J)$, and therefore make the same choice for all field functions.

The question then arises regarding the values taken by the arguments $\hat{X}_j$. Since all field functions belong to the space H^+, all arguments $\hat{X}_j$ must satisfy the inequality

$$\mathrm{Im}\{\hat{X}_j\} = \mathrm{Im}\{\xi + m_j\hat{\gamma}_j z + \hat{\eta}_j\} \geq 0. \tag{21}$$

This condition is achieved by an appropriate choice of the delay $\hat{\eta}_j$. In practice, this delay is calculated so that the z-coordinate in the expression for $\hat{X}_j$ vanishes on the interface from which the plane wave originates, regardless of whether the wave is propagating or evanescent. This practice is common for monochromatic fields, although it is not essential in this case since the upper and lower parts are entire functions. Nevertheless, it improves the conditioning of numerical computing.

Thus, the set of interface conditions (14) can be expressed in terms of complex fields as

$$I\left\{\hat{f}_0^+(X_0),\ \hat{f}_1^+(\hat{X}_1),\ \ldots,\ \hat{f}_J^+(\hat{X}_J)\right\} = 0. \tag{22}$$

Back to real physical fields. Since the signal function $f_0(X)$ of the incident field is real for real X, according to (8), the corresponding physical field is given by

$$\varphi_{0\mathrm{inc}} = f_0(X_0) = 2\mathrm{Re}\left\{\hat{f}_0^+(X_0)\right\}. \tag{23}$$

Now, since the operator I has real coefficients, it follows from Eq. (22) that the linear system

$$I\left\{2\mathrm{Re}\left[\hat{f}_0^+(X_0)\right],\ 2\mathrm{Re}[\hat{f}_1^+(\hat{X}_1)],\ \ldots,\ 2\mathrm{Re}[\hat{f}_J^+(\hat{X}_J)]\right\} = 0 \tag{24}$$

holds. Solving the system yields the unknown functions $\hat{f}_j^+(X_j)$, $(j = 1, \ldots, J)$, and the corresponding physical field solutions of the interaction problem associated with the incident field (23) are then given by

$$\varphi_j = 2\mathrm{Re}\left\{\hat{f}_j^+(\hat{X}_j)\right\},\ (j = 1, \ldots, J). \tag{25}$$

It is worth noting that the formalism is applicable for elastic solid media, both isotropic and anisotropic; the governing equations are actually more complex than in the fluid case and require the simultaneous treatment of displacement and stress fields. In particular, the present formalism allows one to address phenomena such as transient Rayleigh waves and to analyze particle motion depending on the nature of the incident transient signal.

A. Summary of Sec. III

For a multilayered propagation domain, separated by parallel interfaces, the propagation equations for the various waves in each medium, together with the continuity conditions at each interface, form a linear differential system with real coefficients: the system [(13), (14)]. This system is then expressed in terms of complex fields, namely, the upper parts of the signal functions describing each field. The system is subsequently solved (iteratively in the case of multiple interfaces) for a given input function (incident wave). The solutions for the unknown fields appear as complex-valued functions whose argument is real for propagative waves and complex for evanescent fields. Since the physical incident wave is represented by a real-valued function $f(X)$, it follows from the properties of the linear system and from relation (8) that the physical solutions for the other fields are obtained by taking the real part of their upper parts, which solve the system, according to Eq. (25).

IV. A BROAD CLASS OF DECOMPOSABLE FUNCTIONS

As a first simple example of decomposable functions $f(X)$ with the analytic extension $f(Z)$, we can consider trigonometric functions. For instance, the analytic decomposition of the cosine function is

$$\cos(KZ) = \exp(iKZ)/2 + \exp(-iKZ)/2, \quad \text{with } K > 0. \tag{26}$$

Any sum of such trigonometric functions belongs to H, for example, the partial sums of Fourier series. More generally, due to the properties of the exponential function, any polynomial of several variables Y_j, with $Y_j = \cos(K_j Z + \theta_j)$, also belongs to H.

A second basic example is the rational function

$$\frac{1}{Z^2+1} = \frac{i}{2}\frac{1}{Z+i} - \frac{i}{2}\frac{1}{Z-i}. \tag{27}$$

More generally, any rational function with no real poles and no entire part belongs to the space H of decomposable functions. The decomposition of such a rational function can be easily obtained by separating the singular parts of its poles with positive imaginary parts from those with negative imaginary parts. A generalization to certain meromorphic functions in the plane $\mathbb{C}$ is possible by applying the Mittag–Leffler theorem (see Ref. 16, chapter 5, Sec. 2.1). For example, the function $1/\cosh(KZ)$ is analytically decomposable.

Using a procedure frequently employed in the Wiener–Hopf technique (see Refs. 9–11), we may combine the two previous sets of decomposable functions [(26), (27)] by considering their products. For instance, we may write

$$\frac{\cos(KZ)}{Z^2+1} = \frac{i}{4}\left\{\frac{\exp(iKZ)}{Z+i} + \frac{\exp(-iKZ)}{Z+i} - \frac{\exp(iKZ)}{Z-i} - \frac{\exp(-iKZ)}{Z-i}\right\}, \tag{28}$$

where the first term in the braces belongs to H^+ and the last term to H^-, while the intermediate terms are mixed. To obtain the complete decomposition, we rewrite (28) in the following form:

$$\frac{\cos(KZ)}{Z^2+1} = \frac{i}{4}\left\{\frac{\exp(iKZ)+\exp(-K)}{Z+i} - \frac{\exp(iKZ)-\exp(-K)}{Z-i} + \frac{\exp(-iKZ)-\exp(-K)}{Z+i} - \frac{\exp(-iKZ)+\exp(-K)}{Z-i}\right\}, \tag{29}$$

where the first two terms belong to H^+ and the last two belong to H^-.

By generalizing this procedure, we see that any product of a polynomial function of trigonometric arguments with a rational function satisfying the prescribed conditions belongs to the space H, as does any sum of such products. Therefore, we obtain a broad class of analytically decomposable functions that allow accurate modeling of most real signals.

Example. A transient monochromatic wave train may be modeled by the field function

$$f(Z) = \cos(KZ)/(Z^n+1), \quad \text{with } K > 0 \text{ and } n \text{ an even integer.} \tag{30a}$$

For sufficiently large n, the rational function provides a good analytic approximation of the rectangular function on the interval $[-1, 1]$.

In expression (30a), the argument Z should be understood as a dimensionless time related to a reference time t_0, which sets the (approximate) total duration $2t_0$ of the signal. Expressed in terms of the real dimensionless variable $Z = X$, this duration is equal to 2 in Fig. 1(a). Apart from the π factor, the parameter $K = 2\pi t_0/T$ represents the number of periods of the sinusoidal term over this total duration.

By extending the result (29), the upper part of the function (30a) can be expressed in the form

$$\hat{f}^+(Z) = -\frac{1}{2n}\sum_{p=1}^{n/2}\left\{\frac{Z_p}{Z-Z_p}[\exp(iKZ) - \exp(iKZ_p)] + \frac{Z_p^*}{Z-Z_p^*}\left[\exp(iKZ) - \exp(-iKZ_p^*)\right]\right\}, \tag{30b}$$

where the poles Z_p are given by $Z_p = \exp[i\pi(2p-1)/n]$ with $(p = 1, \ldots, n/2)$. Recall that Z_p^* denotes the complex conjugate of Z_p.

As examples, Figs. 1(a) and 1(b) show the field function (30b) for $(n = 60,\ K = 50)$ and $(n = 2,\ K = 10)$, respectively, while

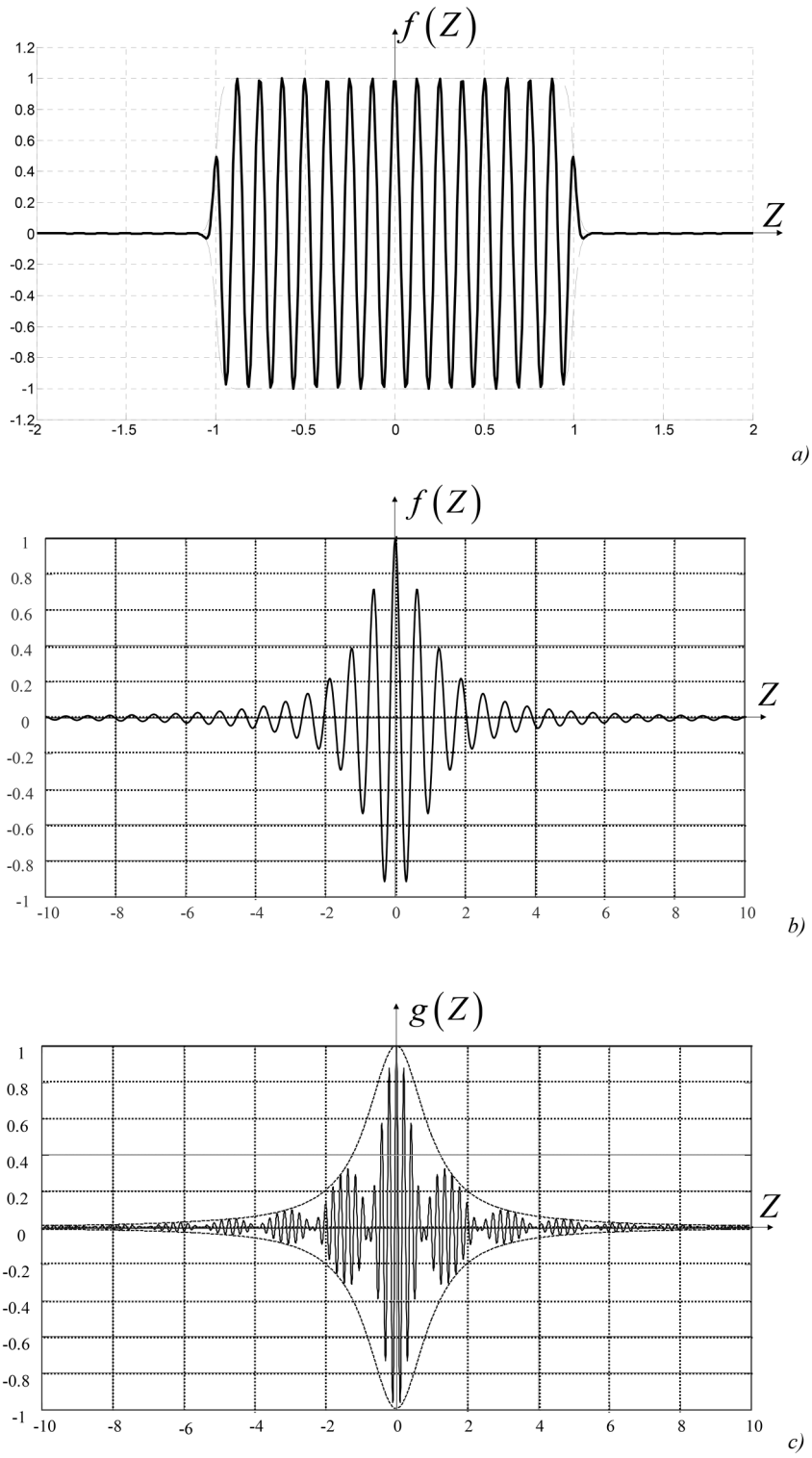

FIG. 1. The signal function as a function of the dimensionless variable Z. (a) Signal function (30a), $n = 60$, $K = 50$. (b) Signal function (30a), $n = 2$, $K = 10$. (c) Signal function (31) with beat oscillations, $n = 2$, $K_1 = 30$, $K_2 = 2$.

Fig. 1(c) shows the field function

$$g(Z) = \cos(K_1 Z)\cos(K_2 Z)/(Z^n + 1), \quad \text{with } K_1 > 0,\ K_2 > 0 \text{ and } n \text{ an even integer}, \tag{31}$$

which exhibits a slowly varying profile ($n = 2$) with beating oscillations ($K_1 = 30$, $K_2 = 2$). Note that Fig. 1(b) shows the incident signal used in both Figs. 3(a) and 3(b).

Besides this direct determination of the analytic decomposition, which applies to this broad class of functions, the classical Fourier transform method used in signal processing remains available for other functions, provided they admit a Fourier transform. Among these are functions that are only piecewise analytic; however, in such cases, the uniqueness of the decomposition is not guaranteed.

It should be emphasized that the analytic functions discussed herein are dense (in some mathematical sense) in the set of piecewise continuous functions. Namely, these infinitely differentiable analytic functions make it possible to regularize the pulse functions commonly used in integral methods. Furthermore, the use of analytic functions avoids the need for windowing procedures commonly employed in signal processing—which are inherently non-analytic—to remove discontinuities. It should also be emphasized that the proposed method applies to deterministic fields that can be represented as a superposition of plane waves, such as transducer-generated fields (plane waves or beams).

The explicit computations involved in the paper rely exclusively on analytic functions that are directly available in standard scientific software, which greatly facilitates numerical implementation and ensures both robustness and efficiency. In practice, all quantities are evaluated from closed-form expressions derived analytically.

A. Summary of Sec. IV

The vector space of functions constructed in this section satisfies the hypotheses of Sec. II. These functions allow one to represent a wide range of physical signals. Moreover, for an appropriate choice of their parameters, they can accurately describe theoretical signals commonly introduced in classical studies. Their main advantage is that they possess an analytical decomposition that can be determined in explicit form. The solution method described in Sec. III then yields explicit expressions for each of the fields involved, in particular, for the evanescent fields. In the Secs. II and III, as an illustration, the method is applied to the case of a planar fluid–fluid interface. The case of a signal close to a rectangular pulse, possibly oscillatory, is presented in detail.

V. SOLVING A TRANSIENT PLANE WAVE PROBLEM

To illustrate the theory outlined above in more detail, as clearly and pedagogically as possible, we consider the interaction of an acoustic transient plane wave with a fluid/fluid interface (see Fig. 2) (more complex configurations, including multilayered and solid media, are left for future studies). The physical parameters of the media F_0 and F_1 are defined as follows ($j = 0, 1$): densities ρ_j,

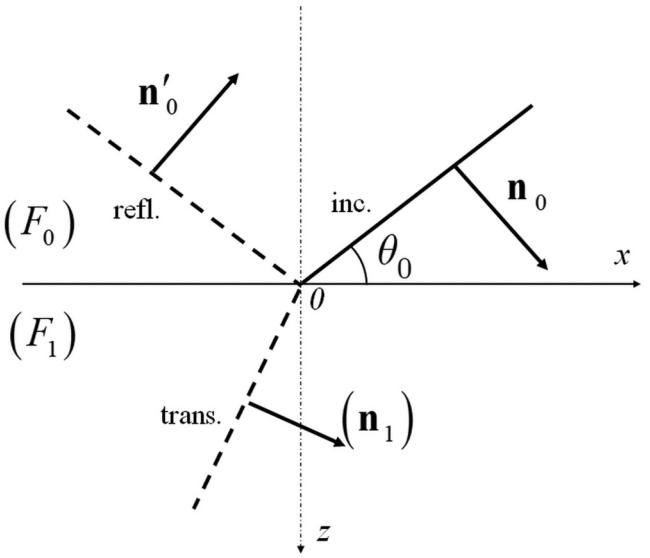

FIG. 2. Geometry of the interaction problem.

sound velocities c_j with $c_0 < c_1$, and slownesses m_j, where

$$m_j = 1/c_j. \tag{32}$$

The problem is two-dimensional. The plane wavefronts are shown in Fig. 2: a solid line for the incident wave and dotted lines for the reflected and transmitted waves. The vectors perpendicular to these planes, namely, $\mathbf{n}_0$, $\mathbf{n}'_0$, and $\mathbf{n}_1$, are the unit propagation vectors [with components denoted α_j and γ_j, which correspond to the parameters α and γ of Eq. (1) evaluated for the propagation medium j], and where θ_0 is the incident angle (between the vector $\mathbf{n}_0$ and the z axis). The three fields involved are represented here by their velocity potentials, although they could equivalently be represented by their acoustic pressures (see Sec. VI). The incident field φ_{inc} is described by a given real signal function $f_0(X_0)$ that satisfies hypotheses (a)–(c) of Sec. II B, with the complex extension $\hat{f}_0(Z)$ and the upper part $\hat{f}_0^+(Z)$, so that we may write

$$\varphi_{\text{inc}} = \text{Re}\{\hat{\varphi}_{\text{inc}}\},\ \hat{\varphi}_{\text{inc}} = 2\hat{f}_0^+(X_0), \quad X_0 = m_0(\alpha_0 x + \gamma_0 z) - t,\ \alpha_0^2 + \gamma_0^2 = 1. \tag{33a}$$

Similarly, the reflected and transmitted fields φ_{ref} and φ_{tra} are sought in the form

$$\varphi_{\text{ref}} = \text{Re}\{\hat{\varphi}_{\text{ref}}\},\ \hat{\varphi}_{\text{ref}} = 2\hat{g}_0^+(X'_0), \quad X'_0 = m_0(\alpha'_0 x + \gamma'_0 z) - t,\ \alpha_0'^2 + \gamma_0'^2 = 1, \tag{33b}$$

$$\varphi_{\text{tra}} = \text{Re}\{\hat{\varphi}_{\text{tra}}\},\ \hat{\varphi}_{\text{tra}} = 2\hat{f}_1^+(\hat{X}_1), \quad \hat{X}_1 = m_1(\alpha_1 x + \hat{\gamma}_1 z) - t,\ \alpha_1^2 + \gamma_1^2 = 1, \tag{33c}$$

where we indicate that the component $\hat{\gamma}_1$ may be imaginary by assigning it a hat. The complex functions $\hat{g}_0^+(Z)$ and $\hat{f}_1^+(Z)$ must be determined in terms of the known function $\hat{f}_0^+(Z)$.

First, these three functions satisfy the wave equation in each relevant medium, F_0 or F_1,

$$E_0\left\{\hat{f}_0^+(X_0)\right\} = 0,\ E_0\left\{\hat{g}_0^+(X'_0)\right\} = 0,\ E_1\left\{\hat{f}_1^+(\hat{X}_1)\right\} = 0. \quad (34)$$

Second, they must satisfy the physical conditions along the interface $z = 0$ for all values of (x, t); therefore, we impose the following conditions:

$$m_0\alpha_0 = m_0\alpha'_0 = m_1\alpha_1; \quad (35)$$

from these, we deduce the Snell–Descartes laws of reflection and refraction

$$\alpha'_0 = \alpha_0, \quad \gamma'_0 = -\gamma_0, \quad \alpha_1 = (m_0/m_1)\alpha_0, \quad \hat{\gamma}_1 = \sqrt{1-\alpha_1^2}. \quad (36)$$

We set

$$\xi = m_0\alpha_0 x - t = m_0\alpha'_0 x - t = m_1\alpha_1 x - t, \quad (37)$$

so that the arguments in Eqs. (33) can be written as

$$X_0 = \xi + m_0\gamma_0 z,\ X'_0 = \xi - m_0\gamma_0 z,\ \hat{X}_1 = \xi + m_1\hat{\gamma}_1 z. \quad (38)$$

If the component γ_1 is real, the solution of the interaction problem is obtained by using the real potentials $f_0(X_0)$, $g_0(X'_0)$, and $f_1(X_1)$ directly.

Under the hypothesis $m_0 > m_1$, the coefficient γ_1 becomes imaginary in the case of supercritical incidence: $\hat{\gamma}_1 = i\gamma''_1$ $(\gamma''_1 > 0)$. Solving the problem then requires the use of complex potentials (33).

The pressures and normal velocities are expressed in terms of the velocity potentials through the following derivatives:

$$\hat{p}_{\text{inc}} = 2\rho_0\hat{f}_0^{+\prime}(X_0),\ \hat{p}_{\text{ref}} = 2\rho_0\hat{g}_0^{+\prime}(X'_0),\ \hat{p}_{\text{tra}} = 2\rho_1\hat{f}_1^{+\prime}(\hat{X}_1), \quad (39a)$$

$$\hat{w}_{\text{inc}} = 2m_0\gamma_0\hat{f}_0^{+\prime}(X_0),\ \hat{w}_{\text{ref}} = -2m_0\gamma_0\hat{g}_0^{+\prime}(X'_0),\ \hat{w}_{\text{tra}} = 2m_1\hat{\gamma}_1\hat{f}_1^{+\prime}(\hat{X}_1). \quad (39b)$$

The continuity of total pressures and normal velocities along the interface $z = 0$ leads, after integration, to the two following equations:

$$\rho_0\left[\hat{f}_0^+(\xi) + \hat{g}_0^+(\xi)\right] = \rho_1\hat{f}_1^+(\xi), \quad \forall\xi \in \mathbb{R}, \quad (40a)$$

$$m_0\gamma_0\left[\hat{f}_0^+(\xi) - \hat{g}_0^+(\xi)\right] = m_1\hat{\gamma}_1\hat{f}_1^+(\xi), \quad \forall\xi \in \mathbb{R}. \quad (40b)$$

From these two functional relations, we deduce the unknown functions,

$$\hat{g}_0^+(\xi) = \hat{R}_{01}\hat{f}_0^+(\xi), \text{ with } \hat{R}_{01} = \frac{\rho_1 m_0\gamma_0 - \rho_0 m_1\hat{\gamma}_1}{\rho_1 m_0\gamma_0 + \rho_0 m_1\hat{\gamma}_1}, \quad (41a)$$

$$\hat{f}_1^+(\xi) = \hat{T}_{01}\hat{f}_0^+(\xi), \text{ with } \hat{T}_{01} = \frac{2\rho_0 m_0\gamma_0}{\rho_1 m_0\gamma_0 + \rho_0 m_1\hat{\gamma}_1}. \quad (41b)$$

The reflection and transmission coefficients $\hat{R}_{01}$ and $\hat{T}_{01}$ do not depend on the choice of the incident signal function; therefore, they have the same expressions as in the monochromatic case. They are complex in the supercritical situation.

Following the procedure presented in Sec. III, we complete the resolution by taking the real parts of the complex potentials just determined. Thus, the physical velocity potentials are given by

$$\hat{\varphi}_{\text{inc}} = 2\hat{f}_0^+(X_0) \Rightarrow \varphi_{\text{inc}} = \text{Re}\{\hat{\varphi}_{\text{inc}}\} = f_0(X_0), \quad (42a)$$

$$\hat{\varphi}_{\text{ref}} = 2\hat{R}_{01}\hat{f}_0^+(X'_0) \Rightarrow \varphi_{\text{ref}} = \text{Re}\{\hat{\varphi}_{\text{ref}}\} = \text{Re}\left\{2\hat{R}_{01}\hat{f}_0^+(X'_0)\right\}, \quad (42b)$$

$$\hat{\varphi}_{\text{tra}} = 2\hat{T}_{01}\hat{f}_0^+(\hat{X}_1) \Rightarrow \varphi_{\text{tra}} = \text{Re}\{\hat{\varphi}_{\text{tra}}\} = \text{Re}\left\{2\hat{T}_{01}\hat{f}_0^+(\hat{X}_1)\right\}. \quad (42c)$$

Note that the decomposition formalism can be applied to both subcritical and supercritical incidences, which may be useful in the case of multilayered media.

Regarding Eqs. (42b) and (40b), we observe that the argument X'_0 of the reflected field is real. Therefore, according to Eq. (12), the potential φ_{ref} can be expressed in terms of the real signal function $f_0(X)$ and its real Hilbert transform $f_{0H}(X)$, namely,

$$2f_0^+(X'_0) = f_0(X'_0) + if_{0H}(X'_0). \quad (43)$$

In this form, the expression (42b) of the reflected field is identical to that available in the literature using Fourier transforms, for the case of a single rectangular signal (see Ref. 1, Sec. 3.6.2), a result to which we will return at the end of Sec. VI.

On the other hand, since the argument $\hat{X}_1$ is complex with $\text{Im}\{\hat{X}_1\} \geq 0$, writing the transmitted field (42c) in a form similar to (43) requires the use of the complex extension $\hat{f}_0(Z)$ of $f_0(X)$, as well as the complex Hilbert transform $\hat{f}_{0\hat{H}}(Z)$ defined by Eq. (9). In fact, we can write

$$2\hat{f}_0^+(\hat{X}_1) = \hat{f}_0(\hat{X}_1) + \hat{f}_{0\hat{H}}(\hat{X}_1). \quad (44)$$

However, this latter relation is only valid in a band $|\text{Im}\{\hat{X}_1\}| < \varepsilon$ of the Z-plane. Consequently, to cover all the values taken by the argument $\hat{X}_1$, it is necessary to use the analytic decomposition method presented above.

VI. EXPLICIT RESULTS

In this section, we adopt the following dimensionless values for the physical parameters of the media F_0 and F_1:

$$m_0 = 1,\ m_1 = 0.3,\ \rho_0 = 1,\ \rho_1 = 2. \quad (45)$$

The component value $\alpha_0 = \sin\theta_0$, where θ_0 is the incident angle, is $\alpha_{0c} = m_1/m_0 = 0.3$ (i.e., $\theta_{0c} \cong 17.5°$) at critical incidence. In the supercritical case, the calculations are carried out

using $\alpha_0 = 0.5$. The three fields are defined here by their acoustic pressures p_{inc}, p_{ref}, and p_{tra}, which satisfy continuity conditions across the interface. The incident pressure is represented by the signal function $f_0(X) = f(X, K, n)$, as defined in Eq. (30a). The pressure fields are then given by Eqs. (42), rewritten in the form

$$p_{inc} = f_0(X_0) = \mathrm{Re}\{\hat{p}_{inc}\},\ \hat{p}_{inc} = 2\hat{f}_0^+(X_0), \tag{46a}$$

$$p_{ref} = \mathrm{Re}\{\hat{p}_{ref}\},\ \hat{p}_{ref} = 2\hat{R}_{01}\hat{f}_0^+(X'_0), \tag{46b}$$

$$p_{tra} = \mathrm{Re}\{\hat{p}_{tra}\},\ \hat{p}_{tra} = 2\hat{T}_{p01}\hat{f}_0^+(\hat{X}_1), \tag{46c}$$

with the transmission coefficient $\hat{T}_{01}$ replaced by $\hat{T}_{p01} = (\rho_1/\rho_0)\hat{T}_{01}$ in Eq. (46c). The arguments X_0, X'_0, and $\hat{X}_1$ are given by Eq. (38). The components $\hat{u}$ and $\hat{w}$ of the particle velocity vector along the x and z axes, respectively, are deduced from the corresponding pressure using the admittance relations, which are obtained from Euler's equation,

$$\hat{u} = [\alpha/(\rho c)]\,\hat{p},\ \hat{w} = [\hat{\gamma}/(\rho c)]\,\hat{p}. \tag{47}$$

A. Physical fields representations

In the following, we shall use maps to present results (Figs. 3, 4, and 6), as in a previous paper,[17] and occasionally we shall examine details by using cuts on these maps (Figs. 5, 7, and 8) to focus on specific features. The upper part of the maps ($z < 0$) represents the fluid medium F_0, where the incident wave and the reflected wave propagate, while the lower part ($z > 0$) represents the semi-infinite fluid medium F_1, where the propagative or evanescent transmitted field, generated at the plane interface $z = 0$ between the two media, propagates. The black arrows, perpendicular to the plane of the longitudinal waves, indicate the direction of propagation. The x axis lies along the interface, with its origin arbitrarily set at the middle of the impact zone where the incident wave interacts with the interface. The maps are understood to represent the fields at a fixed time (at $t = 0$, for example). As time increases, the set of fields progresses without deformation toward $x > 0$.

As a first application of the model discussed above, the incident, reflected, and transmitted pressure fields are represented in Fig. 3(a) for the subcritical case ($\theta_0 = 15°$) and in Fig. 3(b) for the supercritical case ($\theta_0 = 30°$), both with $K = 10$ and $n = 2$. Actually, in the subcritical case, the fields here are expressed by the same real functions as in the classical model, whereas in the supercritical case, they necessarily involve complex functions, which can be modeled using the analytic decomposition method presented above.

Moreover, Fig. 4 shows the pressure fields for a limited-time sinusoidal source that rises and shuts off suddenly (a quasi-rectangular modulation profile, with $n = 1000$). Figure 4(a) includes approximately three periods of a monochromatic signal ($K = 10$), while Fig. 4(b) shows roughly 15 periods ($K = 50$). Within the interval where the field is nonzero, it behaves like a quasi-monochromatic field, as expected. Note that the amplitude fluctuations along the interface of the transmitted fields are not diffraction effects but oscillations similar to those in the incident and reflected fields and that their penetration depth along the z axis varies inversely with frequency: see Figs. 3(b), 4(a), and 4(b), as well as Fig. 5, which shows pressure cuts of the transmitted field extracted from Figs. 3(a) and 3(b); all corresponding to supercritical situations.

B. Comparison with the results in the literature

In order to compare with the results presented a century ago in Ref. 18 and more recently in Refs. 1 and 3 concerning the reflected field, we now consider the particular case of the rectangular signal function. As mentioned above, this function can be described with very high accuracy by the expression given in Eq. (30a) with $K = 0$ and a very large even integer n. Here, we choose $n = 1000$. The function then admits an effective support consisting of the segment $-1 \le X \le 1$, on which it takes the value 1, while being practically zero outside. It is important to remember, however, that the function is analytic on the entire real axis.

In the supercritical case, with an incident angle $\theta_0 = 30°$, so that $\alpha_0 = \sin\theta_0 = 0.5$, the main interaction region with the interface is located on the segment $-2 \le x \le 2$. Note also that the entire phenomenon can be described by assuming $t = 0$, with the understanding that for $t \ge 0$ the interaction zone shifts toward $x > 0$, all else being equal.

Figure 6 shows the pressure field maps in both fluid media. Two cross sections of these fields are shown in Figs. 7 and 8. Figure 7 displays the values along the interface ($z = 0$) for the incident (dashed line) and reflected (solid line) fields. Figure 8 shows a cross section perpendicular to the interface at $x = 4$ (see also Fig. 6), where the incident wave (dashed line) has not yet arrived.

Concerning the reflected field, two observations can be made. The first relates to the amplitude of the wave. For subcritical incidence, the reflected field would have the same shape as the incident field, but with a reduced amplitude. In the supercritical case, however, Fig. 7 shows a noticeably different shape, with cusp-like points at the ends of the interaction (or impact) zone. In Ref. 1, pp. 154–156, the reflected field takes infinite values at the corresponding points. This is due to the Hilbert transform that occurs in the solution and which is singular for the exact rectangular function studied by the author. By contrast, for a function given by Eq. (30a), the Hilbert transform remains analytic for any real value $Z = X$. The reflected field is, thus, indefinitely differentiable at every point, and the two cusp-type points observed are in fact only very narrow extrema.

The second observation concerns the "precursor" phenomenon, reported in the literature[1] as an "apparent paradox," since it propagates in a region of F_0 not yet reached by the incident wave. Indeed, the map in Fig. 6 reveals a more intense line at the front of the reflected wave. This line corresponds to the leading cusp-like point, which is also clearly visible in the cross section of Fig. 6 shown in Fig. 7. Moreover, ahead of this intense line, Fig. 6 shows a portion of the reflected field with lower, but nonzero, intensity. The cut along the interface (Fig. 7) makes it possible to assess the amplitude of this part of the reflected field, called precursor, that

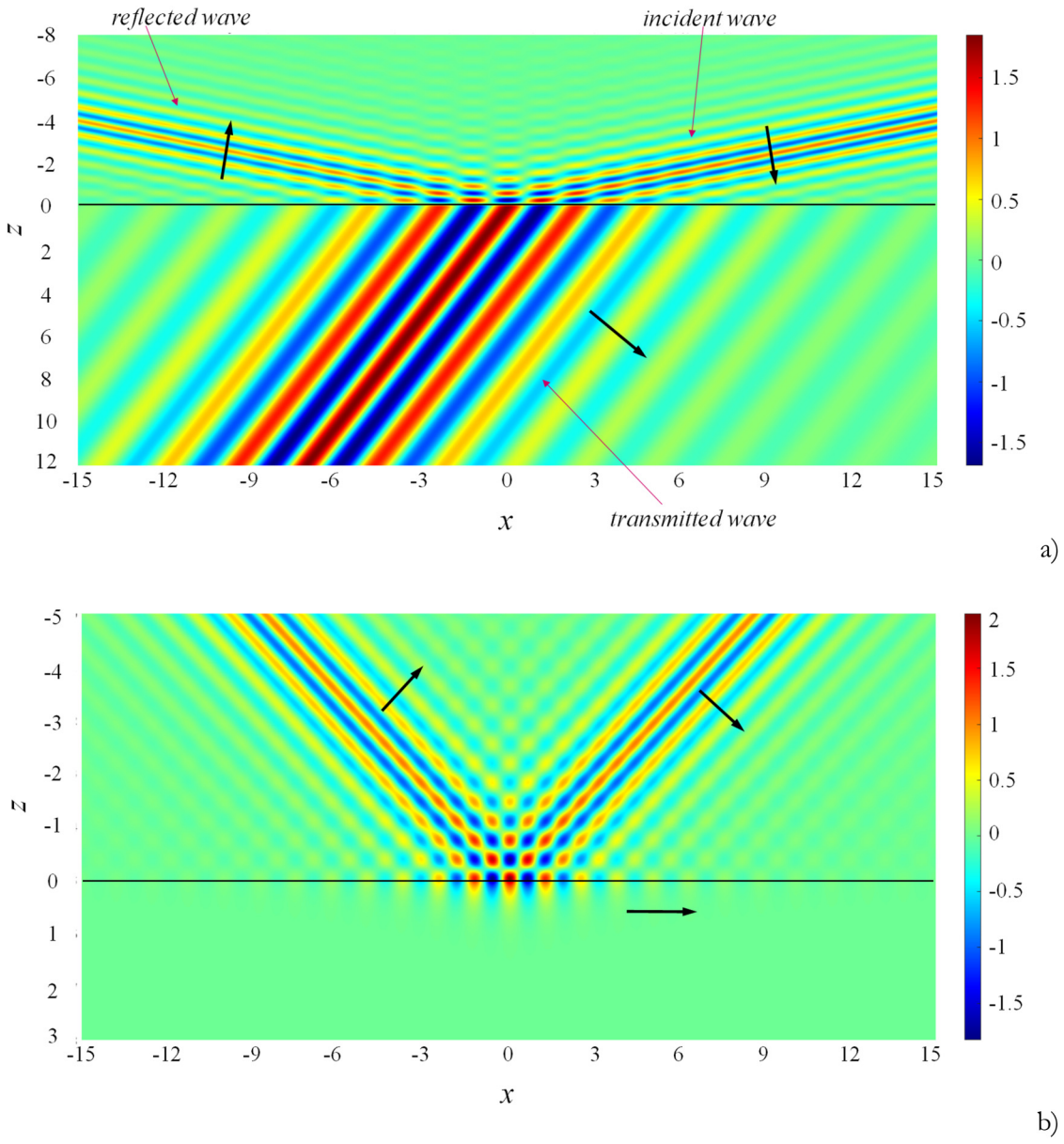

FIG. 3. Pressure field maps for $K = 10$ and $n = 2$. (a) Subcritical case ($\theta_0 = 15°$). (b) Supercritical case ($\theta_0 = 30°$).

precedes the arrival of the incident wave, the amplitude decreasing as one moves away from the impact zone.

The cross section in Fig. 8, perpendicular to the interface in a region not yet reached by the incident wave, also shows the presence of this precursor not only in F_0 medium ($z < 0$) but also in medium $F_1(z > 0)$, where it is of greater intensity. Figure 6 further highlights the region of significant amplitude of the transmitted wave. Along the interface, this region extends beyond the impact interval of the incident wave—upstream, corresponding to the precursor, but also downstream, forming a "successor", just as paradoxical as the precursor. Two arguments can explain these apparent paradoxes.

(i) The first argument is mathematical in nature. In the supercritical case, the wave equation for the transmitted field p_{tra}, expressed in terms of the variables ξ and z, can be written, according to Eqs. (33c) and (38), as

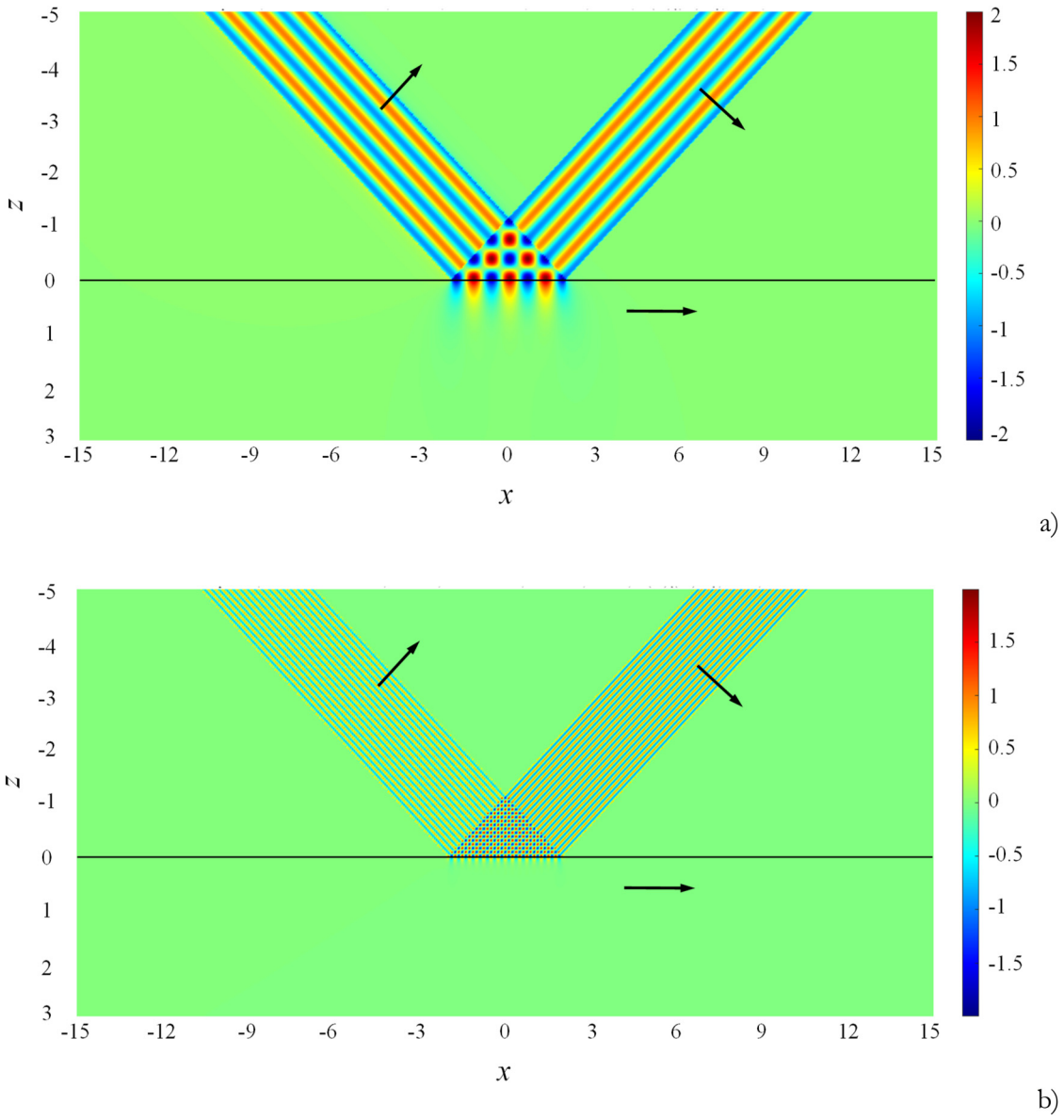

FIG. 4. Pressure field maps for a supercritical case ($\theta_0 = 30°$, $n = 1000$) at two different frequencies: (a) $K = 10$ and (b) $K = 50$.

$$\left(\alpha_1^2 - 1\right)\frac{\partial^2 p_{\text{tra}}}{\partial \xi^2} + \gamma_1'^2 \frac{\partial^2 p_{\text{tra}}}{\partial z^2} = 0. \tag{48}$$

Since we have $\alpha_1 = m_0\alpha_0/m_1 > m_0\alpha_{0c}/m_1 = 1$, Eq. (48) is of elliptic type. Consequently, the solution p_{tra} is analytic in the fluid $F_1(z > 0, \forall\xi)$ and can vanish only at isolated points. In particular, this finite pressure field is present at every point of the interface $(z = 0)$ for any value of ξ, as illustrated in Fig. 8 at abscissa $x = 4$ (for $t = 0$).

(ii) The second argument concerns energy propagation. In Ref. 1, the author explains the apparent paradox of the precursor by invoking the presence of a faster wave propagating in fluid F_1, stating (p. 155): "Since (…) c_1 be greater than c_0, it is possible for acoustic energy to arrive earlier at the listener location via a faster path (…) in the second medium." The explicit solution (46c) for the transmitted field enables us to investigate this issue further. Two questions then arise (see Sec. VI C): What energy exchanges occur between the two fluids? How does energy propagate within fluid F_1?

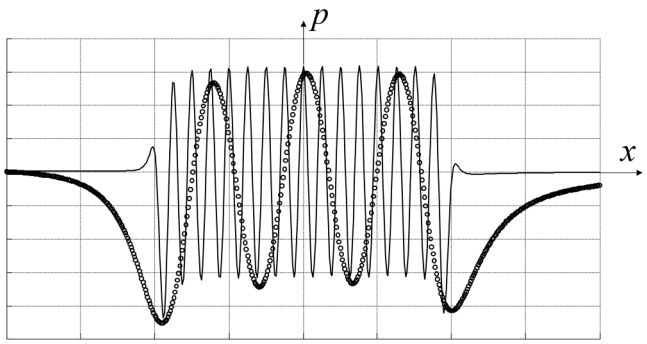

FIG. 5. Pressure cuts of the transmitted field at a depth of $z_1 = 2\pi/K$ for a supercritical case ($\theta_0 = 30°$, $n = 1000$), extracted from Fig. 3(a) for $K = 10$ (circular markers) and from Fig. 3(b) for $K = 50$ (solid line).

C. A modeling approach using energy densities and power fluxes

1. Definition of the energy quantities used

In each fluid medium, the classical "instantaneous" energy quantities (superscript "*ins*"), namely, the energy density E^{ins} and the power flux $\mathbf{F}^{\text{ins}}$, are associated with the real physical fields p, u, and w, and are defined, respectively (see Ref. 2, Sec. 1.4), by the following relations:

$$E^{\text{ins}} = \rho\{u^2 + w^2 + [p/(\rho c)]^2\}/2,$$
$$\mathbf{F}^{\text{ins}} = p\mathbf{v} = \left(F_x^{\text{ins}}, F_z^{\text{ins}}\right) = (pu, pw), \tag{49}$$

where p is the acoustic pressure and $\mathbf{v}$ is the particle velocity vector, with components (u, w) along the Ox and Oz axes, respectively. These quantities satisfy the conservation equation

$$\frac{\partial E^{\text{ins}}}{\partial t} + div(\mathbf{F}^{\text{ins}}) = 0, \tag{50}$$

from which one can deduce instantaneous energy propagation speed $\mathbf{W}^{\text{ins}}$, defined as the ratio

$$\mathbf{W}^{\text{ins}} = \mathbf{F}^{\text{ins}}/E^{\text{ins}}. \tag{51}$$

When these physical fields are expressed using complex fields, as in Eqs. (46), let for the pressure $p = \text{Re}(\hat{p}) = (\hat{p} + \hat{p}^*)/2$, the instantaneous quantities can be written as the sum of two terms, for example,

$$pu = (\hat{p} + \hat{p}^*)(\hat{u} + \hat{u}^*)/4 = (\hat{p}\hat{u}^* + \hat{p}^*\hat{u})/4 + (\hat{p}\hat{u} + \hat{p}^*\hat{u}^*)/4.$$

These two terms are called the "active" and the "complementary" corresponding quantities, respectively. They are denoted by the superscripts "*act*" and "*com*":

$$E^{\text{ins}} = E^{\text{act}} + E^{\text{com}}, \ \mathbf{F}^{\text{ins}} = \mathbf{F}^{\text{act}} + \mathbf{F}^{\text{com}}. \tag{52}$$

The "active" energy quantities, given by the expressions

$$E^{\text{act}} = \frac{\rho}{4}\left\{\hat{u}\hat{u}^* + \hat{w}\hat{w}^* + \frac{\hat{p}\hat{p}^*}{(\rho c)^2}\right\},$$
$$\mathbf{F}^{\text{act}} = \frac{1}{2}\text{Re}\{p\hat{\mathbf{v}}^*\} = \frac{1}{2}\text{Re}(\hat{p}\hat{u}^*, \hat{p}\hat{w}^*) = \left(F_x^{\text{act}}, F_z^{\text{act}}\right), \tag{53}$$

represent the essential contribution of energy. For a monochromatic plane wave, they are associated with the mean values of the

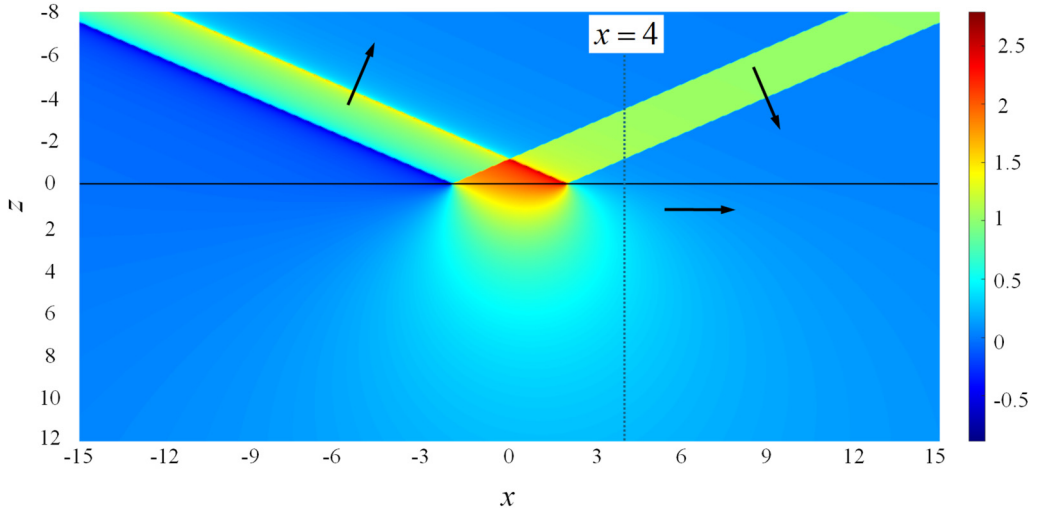

FIG. 6. Pressure field maps for a rectangular signal, supercritical case ($\theta_0 = 30°$, $n = 1000$, $K = 0$).

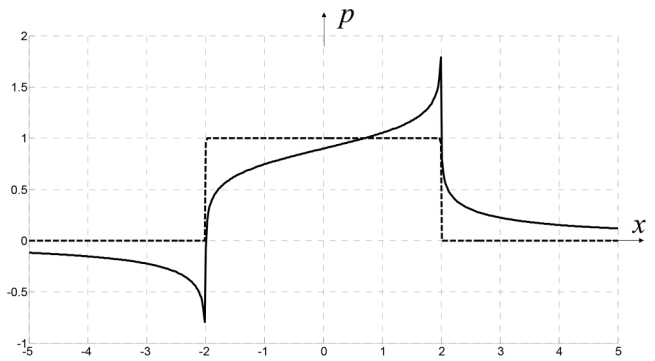

FIG. 7. Incident (dashed line) and reflected (solid line) pressure fields on the interface ($\theta_0 = 30°$, $K = 0$, $n = 1000$).

corresponding quantities; the vector $\mathbf{F}^{\text{act}}$ corresponds to the usual intensity vector $\mathbf{I}$.

The "complementary" energy quantities are expressed as

$$E^{\text{com}} = \frac{\rho}{4}\text{Re}\{\hat{u}^2 + \hat{w}^2 + [\hat{p}/(\rho c)]^2\},$$
$$\mathbf{F}^{\text{com}} = \frac{1}{2}\text{Re}\{\hat{p}\hat{\mathbf{v}}\} = \frac{1}{2}\text{Re}(\hat{p}\hat{u},\ \hat{p}\hat{w}) = \left(F_x^{\text{com}}, F_z^{\text{com}}\right). \tag{54}$$

Each of the two sets of energy quantities, $\{E^{\text{act}}, \mathbf{F}^{\text{act}}\}$ and $\{E^{\text{com}}, \mathbf{F}^{\text{com}}\}$, satisfies a conservation equation of the form of Eq. (50). For both, it is, thus, possible to define the energy propagation speeds by the ratios analogous to Eq. (51): $\mathbf{W}^{\text{act}} = \mathbf{F}^{\text{act}}/E^{\text{act}}$ and $\mathbf{W}^{\text{com}} = \mathbf{F}^{\text{com}}/E^{\text{com}}$.

Note, however, that E^{com} and $\mathbf{F}^{\text{com}}$ are not energy quantities in themselves: they represent local fluctuation of the instantaneous energy. While the energy densities E^{ins} and E^{act} are positive-definite, the complementary energy density E^{com} can change sign. Consequently, the complementary energy propagation speed $\mathbf{W}^{\text{com}}$ is not constrained by the condition $\|\mathbf{W}^{\text{com}}\| \leq c$, and it can even become singular when E^{com} vanishes.

2. Application to the acoustic problem considered

Coming back to the transmitted field, we see readily that in the subcritical case, when the transmitted wave is a propagating plane wave, the three preceding energy quantities propagate with the same velocity, namely, the wave speed $c\,\mathbf{n}$.

The situation is quite different in the supercritical case, where the transmitted field is evanescent. From relations (46), it follows that the z-component of the active energy flux is zero ($F_{z,\text{tra}}^{\text{act}} = 0$), a well-known result in the monochromatic case. In particular, there is no exchange of active energy between the two fluids across the interface, and we have

$$F_{z,\text{tra}}^{\text{ins}} = F_{z,\text{tra}}^{\text{com}}. \tag{55}$$

Thus, our analysis now focuses solely on complementary energy exchanges between the two fluids. Figure 9 shows the variation of the z-component F_z^{com} of the complementary power flux as a function of x on the interface at $z = 0$ (solid line), together with the pressure of the corresponding incident field (dashed line). We observe that F_z^{com} is positive over the main downstream part of the impact zone (for $x \in [-2,\ 0.7]$), where the transmitted wave consequently receives energy from the incident field. Conversely, the power flux is negative (flowing from F_1 toward F_0) in the remaining part $x \in [0.7\,,\ 2]$ of the impact zone and on both sides outside of it (precursor for $x > 2$ and successor for $x < -2$). This flux is relatively larger ahead of the zone than behind it. Thus, outside the impact zone, the transmitted field generates two components of the reflected field: the precursor field and a weaker "successor field", which corresponds to a transient decay of the reflected field.

It is worth verifying that the net balance of these energy exchanges between the two media along the interface is zero. To this end, we must show that the integral of F_z^{com} over the interface

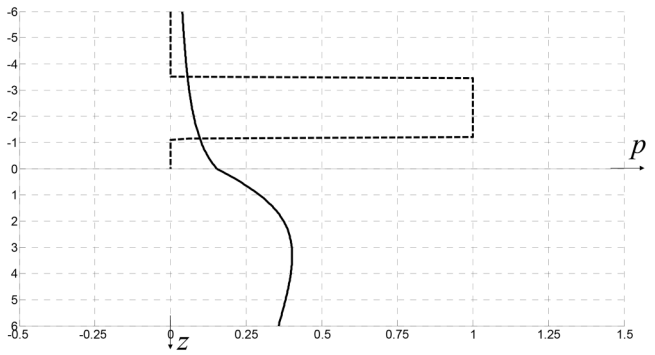

FIG. 8. Cross-sectional representations of the pressure fields at $x = 4$ ($\theta_0 = 30°$, $K = 0$, $n = 1000$): incident (dashed line), reflected (solid line, $z < 0$), and transmitted (solid line, $z > 0$).

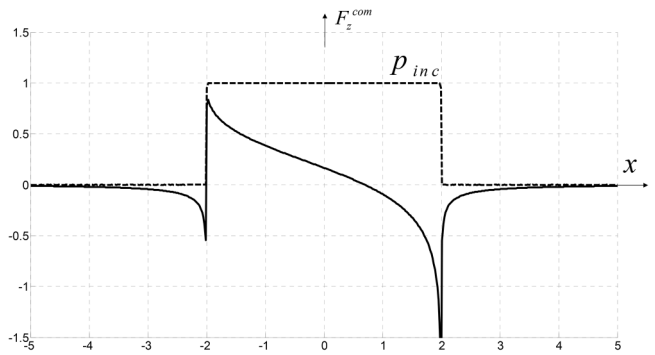

FIG. 9. z-Component F_z^{com} of the complementary power flux as a function of x on the interface at $z = 0$ (solid line) and the related pressure of the incident field (dashed line), for $\theta_0 = 30°$, $K = 0$, and $n = 1000$.

vanishes, namely,

$$\int_{-\infty}^{+\infty} F_{z,\mathrm{tra}}^{\mathrm{com}}(\xi, z=0)d\xi = 0, \tag{56}$$

where ξ is defined in Eq. (16).

From Eqs. (46c) and (47), it follows that

$$F_{z,\mathrm{tra}}^{\mathrm{com}}(\xi, z=0) = \frac{1}{2}\mathrm{Re}(\hat{p}_{\mathrm{tra}}\hat{w}_{\mathrm{tra}}) = 2\frac{m_1}{\rho_1}\mathrm{Re}\left\{\hat{\gamma}_1\hat{T}_{p01}^2\left[\hat{f}_0^+(\xi)\right]^2\right\}. \tag{57}$$

Due to the decay property of the function $\hat{f}_0^+(Z)$ for $\mathrm{Im}\{Z\} \to +\infty$, as expressed under hypothesis (c), we deduce from the Cauchy theorem in a half-plane $\mathrm{Im}\{Z\} > -\varepsilon$ that the following integral vanishes

$$\int_{-\infty}^{+\infty} \left[\hat{f}_0^+(\xi)\right]^2 d\xi = 0, \tag{58}$$

which leads to result (56).

3. Energy propagation velocities

Finally, to complete the validation of the conjecture reported in Refs. 1 and 3, we calculate the propagation velocities of these energies along the interface in the fluid F_1. We have seen that in the subcritical case (Sec. VI C 2), the three energies propagate with the same velocity $c\,\mathbf{n}$. Therefore, for the projection of this common energy velocity vector onto the x axis, we obtain

$$W_x^{\mathrm{ins}} = W_x^{\mathrm{act}} = W_x^{\mathrm{com}} = \alpha_1 c_1, \quad \text{with } \alpha_1 < 1. \tag{59}$$

In the supercritical case, since $\alpha_1 > 1$ and $\hat{\gamma}_1 = i\gamma_1''$, the energy velocities differ significantly both from those in the subcritical case and from each other. From Eqs. (46c) and (47), we obtain the following values for these velocities:

$$W_{x,\mathrm{tra}}^{\mathrm{act}} = c_1/\alpha_1 = c_0/\alpha_0,\ W_{x,\mathrm{tra}}^{\mathrm{com}} = \alpha_1 c_1 > c_1. \tag{60}$$

Finally, since $\alpha_0 < 1 < \alpha_1$, the following ordering relations hold:

$$c_0 < c_0/\alpha_0 = c_1/\alpha_1 = W_{x,\mathrm{tra}}^{\mathrm{act}} < c_1 < \alpha_1 c_1 = W_{x,\mathrm{tra}}^{\mathrm{com}}. \tag{61}$$

So, we see that the active energy propagates along the interface with the phase velocity $W_{x,\mathrm{tra}}^{\mathrm{act}}$ in the Ox direction. This phase velocity is common to both fluids and lies within the interval $[c_0, c_1]$. Note that it also corresponds to the forward speed of the impact zone.

The complementary energy propagates with the same velocity component $W_{x,\mathrm{tra}}^{\mathrm{com}}$ as in the subcritical case [see Eqs. (59) and (60)]; however, this velocity now exceeds the sound speed c_1 of the medium. This does not contradict physical principles since, as noted at the end of Sec. VI C 1, complementary energy is not an autonomous energy like active energy and appears only as an additional term in the expression of the instantaneous energy.

These results lead to the following conclusions. Since we have $W_{z,\mathrm{tra}}^{\mathrm{act}} = 0$, as a consequence of Eq. (55), the active energy in the fluid F_1 propagates parallel to the interface with a constant speed equal to that of the impact zone. Consequently, it cannot be held responsible for the transfer of energy to the precursor energy.

On the other hand, the component of the complementary energy velocity along Ox in the fluid F_1 exceeds the sound speed c_1 in this medium. In this Ox direction, the complementary energy, therefore, propagates faster than the impact zone. The portion of this energy accumulated ahead of the impact zone is reradiated into fluid F_0 and provides the energy required for the propagation of the precursor. Note that this result on the energy propagation velocity is even more striking than the conjecture mentioned above, as the authors' reasoning was primarily based on the sound speed c_1 itself.

a. Final Remarks. To the best of our knowledge, classical theories on precursors in acoustics and electromagnetism mainly interpret these effects within the framework of dispersive media (beams, plates, granular media, ionized gases, etc.) or periodic media, which give rise to complex transient phenomena. The problems considered in the present work are different, in particular, because, at the interface between two media with different physical properties, discontinuities in waves and associated energy velocities occur, and obliquely incident waves may give rise to evanescent transmitted waves. For these reasons, the modeling proposed here is based on a decomposition of energy fluxes within the framework of the analytical model presented previously, specifically adapted to the objective of evaluating energy fluxes across the interface.

In the case of higher-order poles of the signal function, there is a slightly increased algebraic complexity of the implementation. For instance, extending the algebraic manipulation that leads from Eq. (28) to Eq. (29) (illustrated for $n = 2$) to the case of multiple poles requires subtracting a sufficient number of terms from the Taylor expansion of the exponential function in the numerator.

However, since the choice of the signal function is under full control in the proposed framework, such situations can be avoided in practice by selecting appropriate analytic signal representations.

Note that, finally, the results presented in the figures were obtained using MATLAB® on a standard personal computer. Computation times are always shorter than 10 s for the two-dimensional maps (Fig. 6) and are quasi-instantaneous for the one-dimensional curves (Figs. 7–9). Owing to the fully analytic nature of the expressions, issues related to discretization, numerical stability, or convergence do not arise in the usual sense, and the accuracy is limited only by machine precision.

VII. CONCLUSION

Acoustic propagating and evanescent fields—including those considered in this paper, which involve the interaction of plane waves with plane fluid/fluid interfaces—are often treated under the assumption of harmonic variation in fundamental acoustics and its applications. To go further, for fields generated by transient

sources, analytical or numerical time-domain solutions are usually derived from the Fourier transform of frequency-domain solutions.

In the present paper, an alternative, relatively simple procedure—the analytic decomposition—is employed to study such problems, avoiding the explicit calculation of Fourier integrals. The method relies on analytical signal functions, providing a highly accurate approximation of multi-frequency waves with piecewise continuous amplitude modulation profiles. This formulation provides simple expressions for the interaction of a transient plane wave with one or several fluid/fluid interfaces, including transient evanescent modes, and offers deeper physical insight. Numerical results illustrating the properties of transient fields at fluid/fluid interfaces are presented and discussed for a prototype limited-time source, thereby demonstrating that the analytic decomposition is indeed a potentially powerful tool for addressing analytical solutions in such media.

Future work will address problems involving the interactions of transient plane waves with more complex interfaces—solid/solid or solid/fluid interfaces (with isotropic or anisotropic solids) and even stratified media—taking advantage of the simplicity and effectiveness of the method.

AUTHOR DECLARATIONS

Conflict of Interest

The authors have no conflicts to disclose.

Author Contributions

Philippe Gatignol: Conceptualization (lead); Methodology (lead); Software (equal); Writing – review & editing (equal). **Catherine Potel:** Conceptualization (equal); Methodology (equal); Software (equal); Writing – review & editing (equal). **Michel Bruneau:** Conceptualization (equal); Methodology (equal); Writing – review & editing (equal).

DATA AVAILABILITY

The data that support the findings of this study are available from the corresponding author upon reasonable request.

REFERENCES

[1]A. D. Pierce, *Acoustics: An Introduction to Its Physical Principles and Applications*, 3rd ed. (Springer Nature, Switzerland, 2019).
[2]M. Bruneau, *Manuel d'Acoustique Fondamentale* (Hermès, Paris, 1998); *Fundamentals of Acoustics (T. Scelo, Translator and Contributor)* (ISTE, New York, 2006).
[3]M. Born and E. Wolf, *Principles of Optics*, 4th ed. (Pergamon Press, Oxford, 1970).
[4]B. A. Auld, *Acoustic Fields and Waves in Solids* (Wiley, New York, 1973).
[5]*Materials and Acoustics Handbook*, edited by M. Bruneau and C. Potel (ISTE and Wiley, 2009).
[6]L. Brekhovskikh and O. A. Godin, Acoustics of Layered Media I—Plane and Quasi Plane Waves, *Springer Series on Wave Phenomena*, 2nd ed. (Springer-Verlag, Berlin, 1990), Vol. 5.
[7]M. Tygel and P. Hubral, *Transient Waves in Layered Media* (Elsevier, Amsterdam, 1987).
[8]B. F. Cron and A. H. Nuttall, "Phase distortion of a pulse caused by bottom reflection," J. Acoust. Soc. Am. **37**(3), 486–492 (1965).
[9]B. Noble, *Methods Based on the Wiener–Hopf Technique* (Pergamon Press, New York, 1958).
[10]M. Alkinidri, S. Hussain, and A. Nawaz, "Analysis of noise attenuation through soft vibrating barriers: An analytical investigation," AIMS Math. **8**(8), 18066–18087 (2023).
[11]M. Bruneau, P. Gatignol, P. Lanceleur, and C. Potel, *Exercices d'acoustique—Corrigés détaillés. Rappels de cours (Exercices of Acoustics—Detailed Solutions. Course Reminders), Vol. 3: Problèmes avancés (Advanced Exercises)* (Cépaduès Éditions, Toulouse, 2021).
[12]E. J. Beltrami and M. R. Wohlers, *Distributions and Boundary Values of Analytic Functions* (Academic Press, New York, London, 1966).
[13]E. C. Titchmarsh, *The Theory of Functions* (Oxford University Press, 1939).
[14]H. Cartan, *Théorie élémentaire des fonctions analytiques d'une ou plusieurs variables complexes (Elementary Theory of Analytic Functions of One or Several Complex Variables)* (Hermann, Paris, 1961).
[15]M. Lavrentiev and B. Chabat, *Méthodes de la théorie des fonctions d'une variable complexe (Methods of the Theory of Functions of a Complex Variable)* (Edition MIR (URSS), Moscou, 1972).
[16]L. V. Ahlfors, *Complex Analysis* (McGraw-Hill, 1966).
[17]C. Potel, P. Gatignol, and M. Bruneau, "On using heat maps in teaching in acoustics: Interaction of incident plane wave or incident beam with a solid plane structure," J. Acoust. Soc. Am. **152**(2), 754–764 (2022).
[18]J. Picht, "Beitrag zur Theorie der Totalreflexion," Ann. Phys. **395**(4), 433–496 (1929).